Electronic Supplementary Material (ESI) for Lab on a Chip.
This journal is © The Royal Society of Chemistry 2024

Supporting information

Wearable Intelligent Sweat Platform for SERS-AI Diagnosis of Gout

Zhaoxian Chen[1], Wei Wang[1], Hao Tian[1], Wenrou Yu[1], Yu Niu[1], Xueli Zheng[1*], Shihong Liu[2], Li Wang[3], Yingzhou Huang[1*]

1 Chongqing Key Laboratory of Chongqing Key Laboratory of Interface Physics in Energy Conversion, College of Physics, Chongqing University, Chongqing, 400044, China

2 Chongqing University Cancer Hospital, Department of Palliative care, Department of Geriatric Oncology, Chongqing, China

3 Key Laboratory of Optoelectronic Technology and Systems (Ministry of Education), College of Optoelectronic Engineering, Chongqing University, Chongqing 400044, China

*Corresponding authors: zhengxueli0315@cqu.edu.cn (Xueli Zheng); yzhuang@cqu.edu.cn (Yingzhou Huang)

Table of contents：

Supplementary experimental procedures

Materials. Silver nitrate ($AgNO_3$, 99.99%), Nile blue A ($C_{40}H_{40}N_6O_6S$), creatinine ($C_4H_7N_3O$), Uric Acid ($C_5H_4N_4O_3$), urea (H_2NCONH_2), glucose ($C_6H_{12}O_6$), sodium chloride (NaCl), they were purchased from Shanghai Aladdin biochemical Polytron Technologies Inc. (Shanghai, China). Bromocresol green pH indicator solution, Ethylene glycol (EG, $C_2H_6O_2$), polyvinyl pyrrolidone (PVP, (C_6H_9NO) n, M W=130000) were obtained from Shanghai Maclin Biochemical Technology Co., LTD. Synthetic perspiration and phosphate-buffered saline (PBS) were obtained from Shanghai yuan ye Bio-Technology Co., Ltd. The purchased artificial sweat does not contain UA. The organic filter paper was procured from Advantec (grade 5c, USA). PDMS elastomer (Sylgard 184) was purchased from Dow Corning. All chemicals and reagents used in this study were of analytical grade. Medical-grade double-sided adhesive tape (300LSE) was obtained from 3M. Ultrapure deionized (DI) water (18.2 milliohms cm) water was used for all synthetic processes, which was produced using Aquapro AWL-0502-H (Aquapro International Company LLC., Dover, DE).

Preparation of Ag nanowires. $AgNO_3$ solution (5 mL, 1 M) was mixed with PVP solution (36 mL, 0.6 M), the hybrid solution was vigorously stirred for

1min. The 5 mL EG solution was heated for 5 min at 160℃. Subsequently, the hybrid solution was added to the EG solution using a syringe pump with a of 0.5 mL/min flow rate. In the end, the hybrid solution was continuously heated for 60 min at 160℃. The resulting solution was subsequently centrifuged using a centrifuge for 10 min at 6000 rpm.

Characterization of the wearable sensor. Scanning electron microscope (SEM) images were collected with TESCAN MIRA 3FE, and AgNWs dimensions were estimated from SEM images using ImageJ.

Supplementary results and discussion details

Estimated SERS Enhancement Factor (EF)

For simplicity, we used the analytical EF to estimate the SERS platform, which can be calculated using the following equation.

$$EF = \frac{I_{SERS}/C_{SERS}}{I_{bare}/C_{bare}}$$

I_{SERS} means the intensity at 589 cm^{-1} of the Raman signal of NB, which was about 2900.5 counts; C_{SERS} Is a concentration of NB in the presence of AgNWs, the concentration of NB was 1×10^{-12} M. I_{bare} denotes the intensity of NB with concentration C_{bare}, providing the I_{bare} and C_{bare} which were 255.2 counts and 1×10^{-7} M. The EF of AgNWs substrate was calculated to be 1.14×10^{6}[1,2].

Supplementary Figures

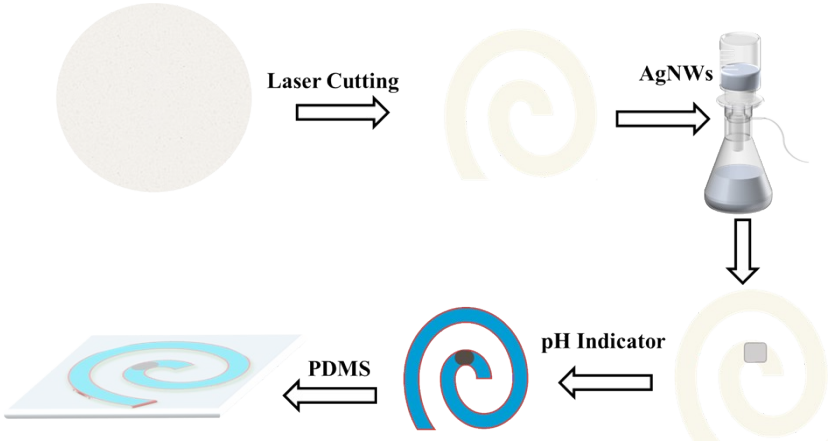

Figure S1. The fabrication process of wearable sweat platform.

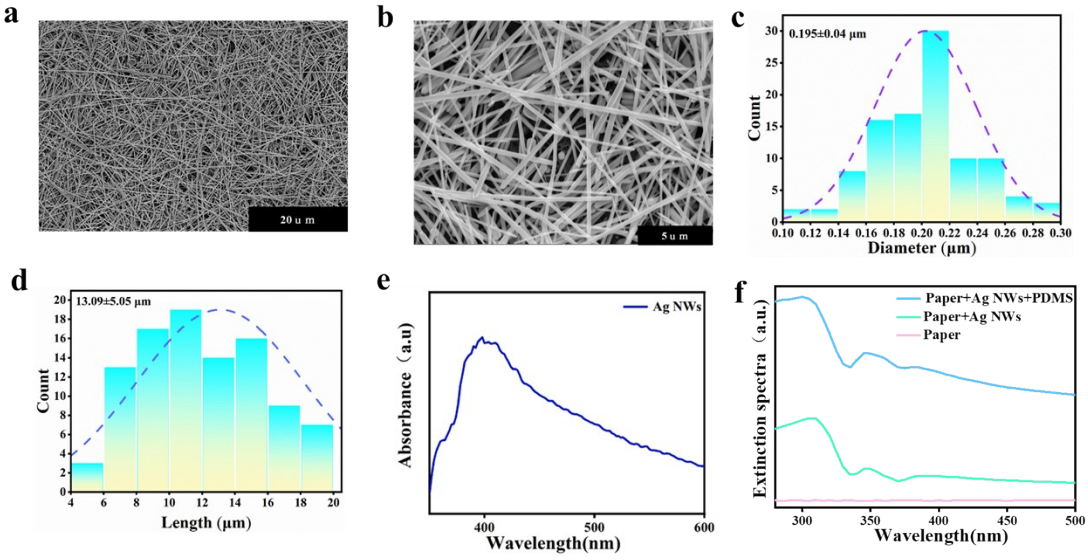

Figure S2. Characterizations of the wearable SERS sensing platform. (a) and (b) SEM images of AgNWs on the paper surface (scale bar: 20 μm and 5 μm).

(c) and (d) Normal distribution histogram of AgNWs with diameter and length. (e) The ultraviolet spectrum of AgNWs solution. (f) The extinction spectrum of paper, AgNWs paper, and AgNWs paper with PDMS.

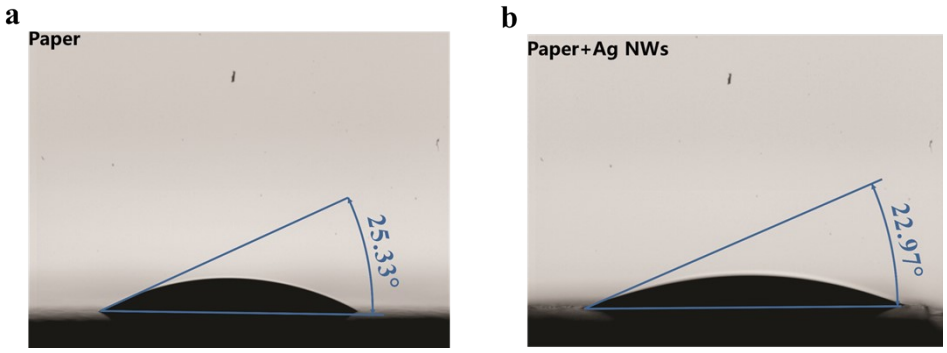

Figure S3. (a) Contact angles of plain filter paper. (b) Contact angles of plain filter paper AgNWs paper.

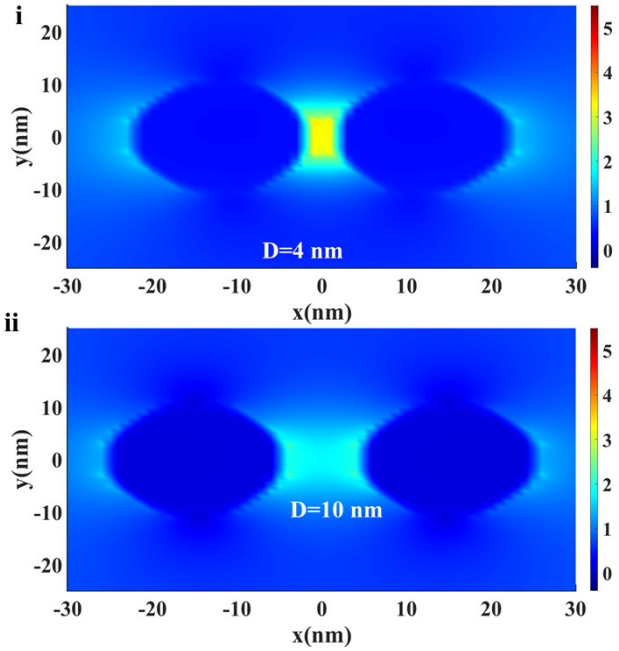

Figure S4. Simulated electric field distribution of AgNW dimer. (i) D=4 nm and (i) D=10 nm.

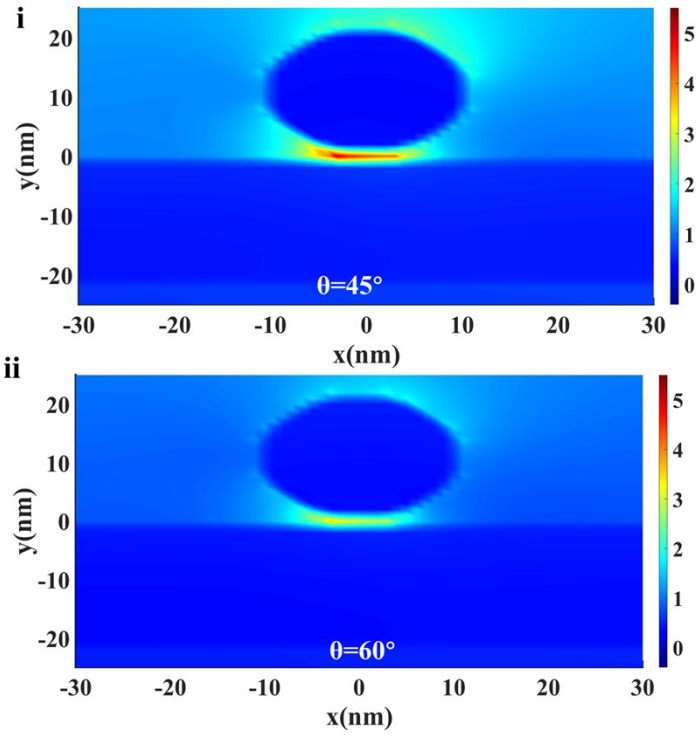

Figure S5. Simulated electric field distribution of AgNW dimer. (i)θ=45° and (ii)θ=60°

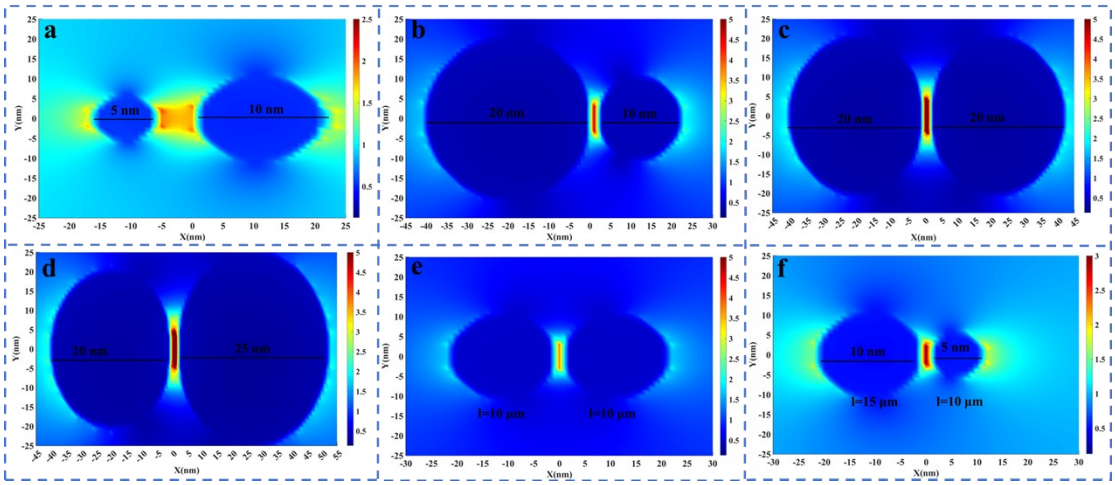

Figure S6. Simulated electric field distribution of AgNW. The different diameter of AgNW, (a) diameter $_1$=5 nm, diameter $_2$=10 nm. (b) diameter $_1$=20

nm, diameter $_2$=10 nm, (c) diameter $_1$=20 nm, diameter $_2$=20 nm, (d) diameter $_1$=20 nm, diameter $_2$=25 nm. The different lengths of AgNW (e) length $_1$=10 μm，length $_2$=10 μm, (f) length $_1$=15 μm，length $_2$=10 μm.

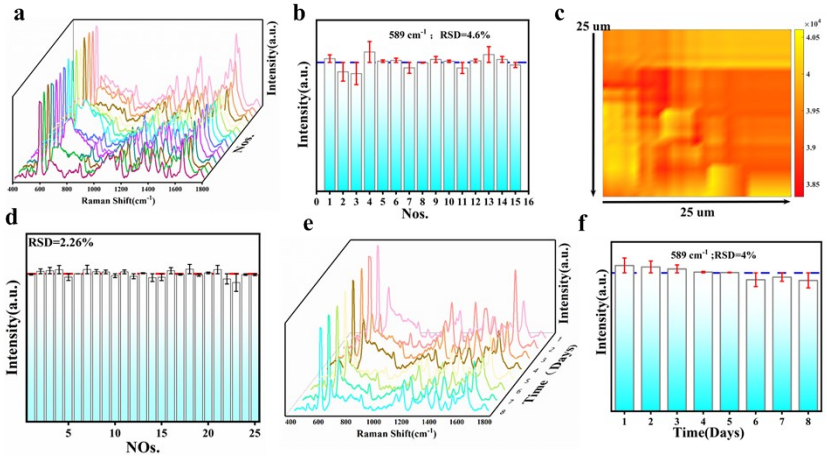

Figure S7. (a) Raman spectra of NB were randomly collected from the AgNWs SERS substrate (n=15). (b) The RSD of the characteristic peak of NB in 589 cm^{-1} form (a). (c) Raman mapping image. (d) The RSD of the characteristic peak of NB in 589 cm^{-1} form (c). (e) Raman spectra NB collected from the first to the eighth day. (f) The RSD of Raman intensities at 589 cm^{-1} at different times.

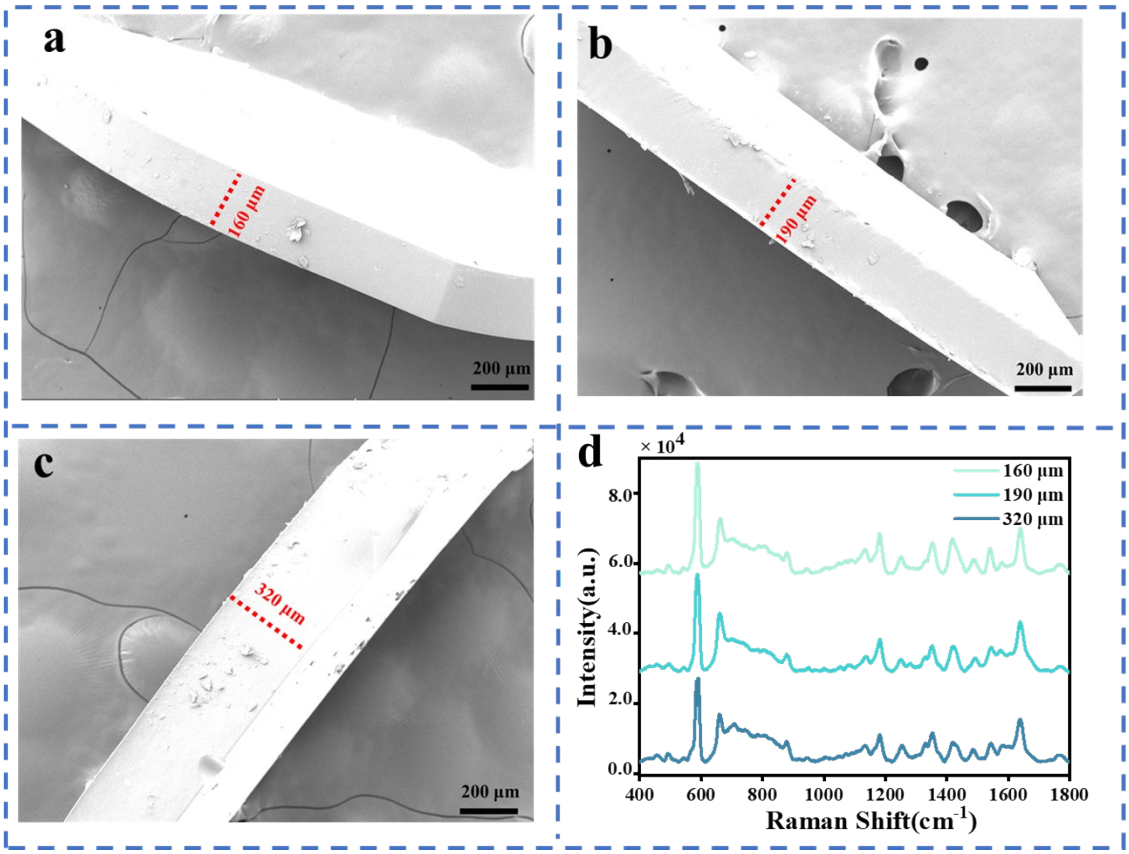

Figure S8. SEM images of the cross-sections of the PDMS films. (a) 160 μm, (b)190 μm, and (c) 320 μm. (d) SERS spectra of 10^{-7} M NB with a PDMS encapsulation layer of varying thicknesses.

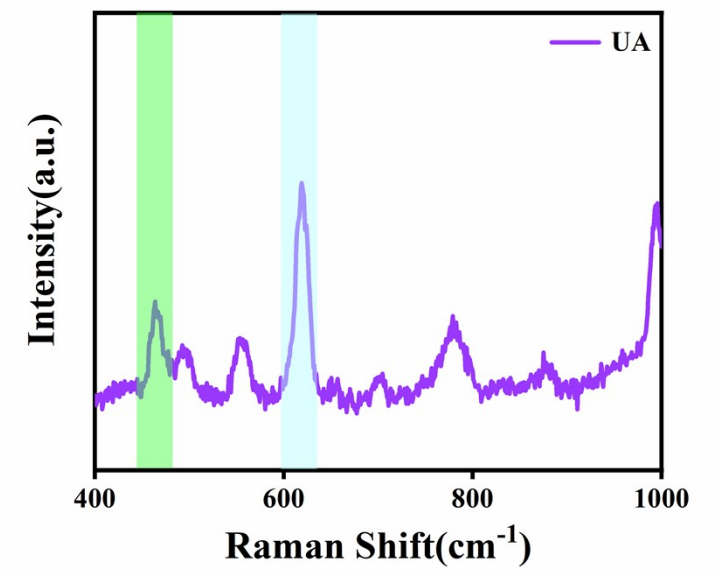

Figure S9. Raman spectra of uric acid.

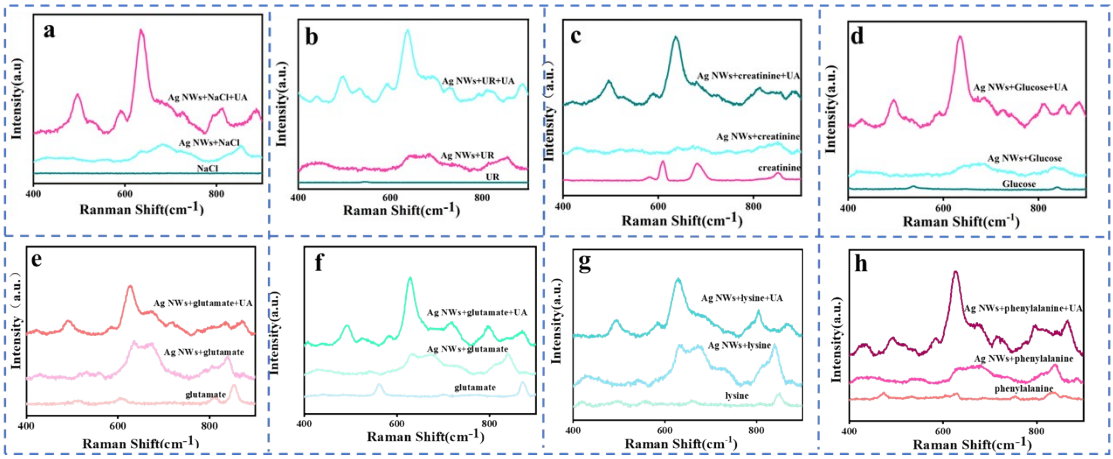

Figure S10. The specificity and selectivity of the SERS platform. Raman spectra of 1×10^{-4} M uric acid and (a) sodium chloride. (b) urea. (c) creatinine. (d) glucose. (e) tyrosine. (f) glutamate.(g) lysine. (h) phenylalanine

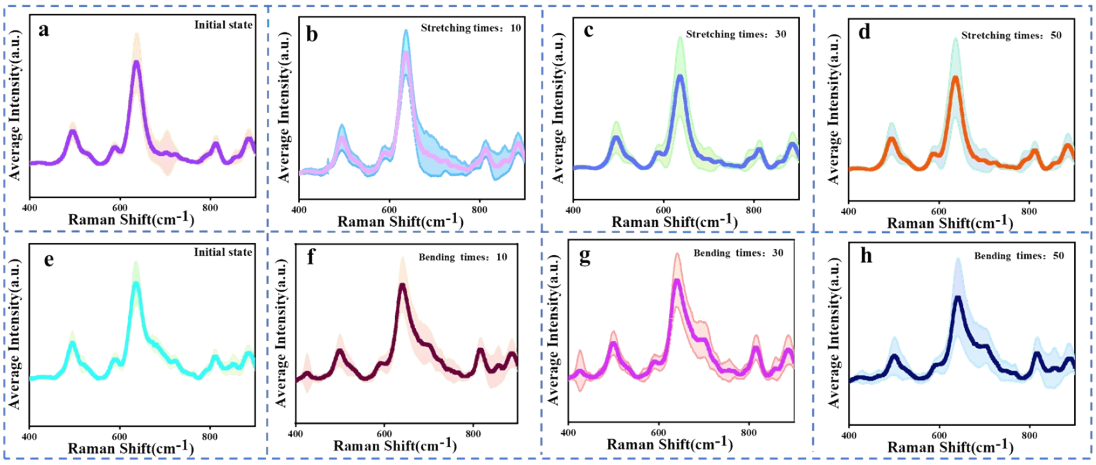

Figure S11. Raman spectra with different number of stretches (a) initial state, (b) 10, (c) 30, (d) 50. Raman spectra with the different number of bends (e) initial state (f) 10, (g) 30, (h)50.

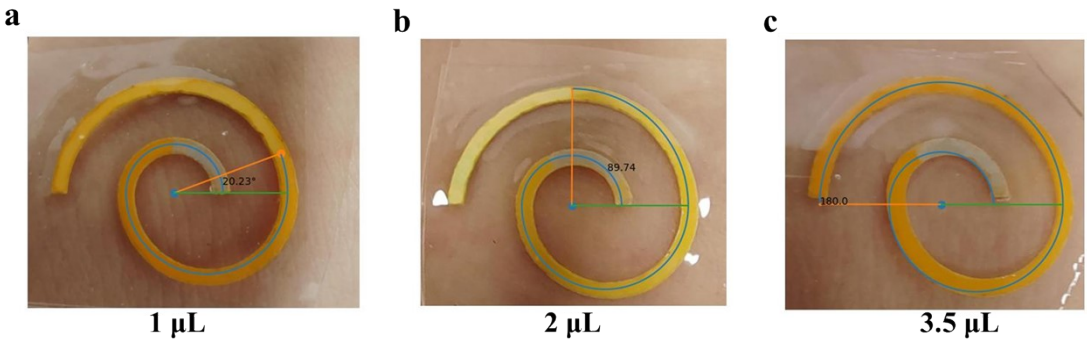

Figure S12. Photographs of the sensor mounted on human skin. Intelligently recognize various volumes of sweat. (a) 1 µL; (b) 2 µL; (a) 3.5 µL;

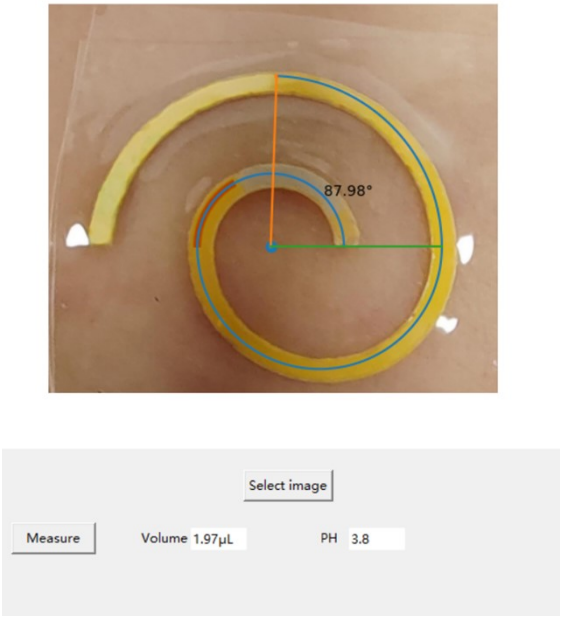

Figure S13. Custom-developed control is interfacial for the sensors.

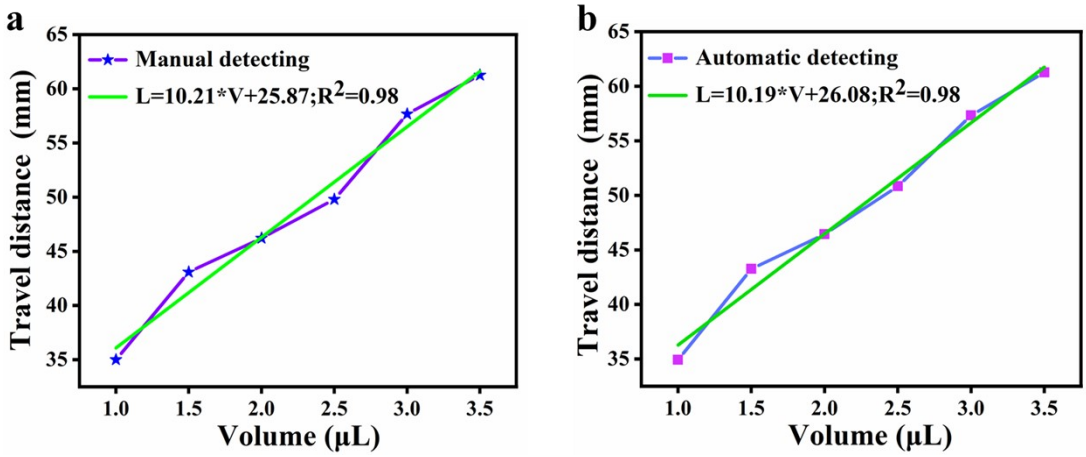

Figure S14. The linear calibration curve of travel distance with the different liquid volumes. (a) Manual detecting and (b) Automatic detecting.

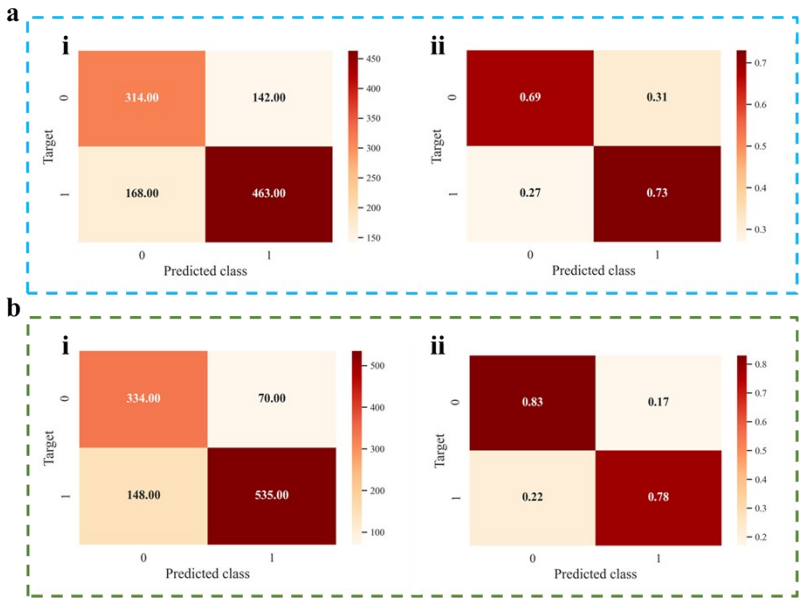

Figure S15. Comparison of prediction performance of PCA and PLS. Confusion matrices of the results predicted by (a) PCA and (b) PLS algorithms

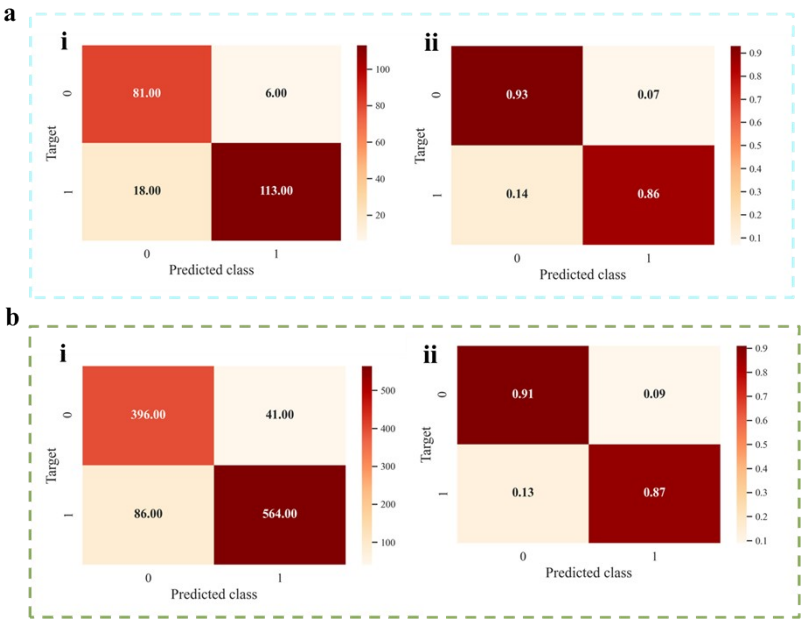

Figure S16. Confusion matrices of the results (a)tested and (b) predicted by ANN algorithm.

Table S1: A comparison with previously published literature for UA detection method.

Year	Periodical	Technology	Analyte	Concentration	Accuracy	Reference
This work		SERS	Uric acid	0.1 μM	97%	This work
2020	Nat. Biotechnol	Electrochemical	Uric acid	0.74 μM	None	[3]
2021	Nano Energy	Electrochemical	Uric acid	10 μM		[4]
2021	Sens. Actuators B Chem.	Electrochemical	Uric acid	1.2 μM		[5]
2022	Anal. Chim. Acta	Electrochemical	Uric acid	2 μM		[6]
2022	ACS Appl. Nano Mater.	Electrochemical	Uric acid	2 μM		[7]
2022	Adv. Mater.	Electrochemical	Uric acid	50-250 μM		[8]

Table S2: A comparison with previously published literature for sweat SERS detection method ingredients.

Year	Periodical	Substrate	Detection substance	Concentration	Accuracy	Reference
This work		Ag NW	Uric acid	0.1 μM	97%	This work
2017	Talanta	Core-shell Au@AgNR	Glucose	None	None	[9]
2021	Anal. Chem	Ag NF	Creatinine & Cortisol	0.106 μM & 0.044 μM		[10]
2021	ACS Appl. Mater. Interfaces	Au/TPU NF	pH	None		[11]
2021	ACS Appl. Mater. Interfaces	Ag NW	2-fluoro-methamphetamine	2.76 μM		[12]
2022	Sens. Actuators B Chem.	Core-shell Au NR	Lactate & Glucose	3.50 mM & 56 mM		[13]
2022	Sci. Adv	Au NR	Uric acid	1 μM		[14]

Supplementary References

1 S. E. J. Bell, G. Charron, E. Cortés, J. Kneipp, M. Lamy de la Chapelle, J. Langer, M. Procházka, V. Tran and S. Schlücker, Angew. Chem. Int. Ed., 2020, 132, 5496–5505.

2 L. Yang, Y. Peng, Y. Yang, J. Liu, H. Huang, B. Yu, J. Zhao, Y. Lu, Z. Huang, Z. Li and J. R. Lombardi, Adv. Sci.,2019,6, 1900310.

3 Y. Yang, Y. Song, X. Bo, J. Min, O. S. Pak, L. Zhu, M. Wang, J. Tu, A. Kogan, H. Zhang, T. K. Hsiai, Z. Li and W. Gao, Nat Biotechnol., 2020, 38, 217–224.

4 X. Wei, M. Zhu, J. Li, L. Liu, J. Yu, Z. Li and B. Ding, Nano Energy, 2021,85, 106031.

5 Z. Xu, J. Song, B. Liu, S. Lv, F. Gao, X. Luo and P. Wang, Sens. Actuators B Chem., 2021,348, 130674.

6 J. Xiao, Y. Luo, L. Su, J. Lu, W. Han, T. Xu and X. Zhang, Anal. Chim. Acta, 2022,1208, 339843.

7 V. Patel, D. Saha, P. Kruse and P. R. Selvaganapathy, ACS Appl. Nano Mater., 2022, 5, 3957–3966.

8 X. Yang, J. Yi, T. Wang, Y. Feng, J. Wang, J. Yu, F. Zhang, Z. Jiang, Z. Lv, H. Li, T. Huang, D. Si, X. Wang, R. Cao and X. Chen, Adv. Mater., 34,2201768.

9 Q. Chen, Y. Fu, W. Zhang, S. Ye, H. Zhang, F. Xie, L. Gong, Z. Wei, H. Jin and J. Chen, Talanta, 2017, 165, 516–521.

10 H. S. Kim, H. J. Kim, J. Lee, T. Lee, J. Yun, G. Lee and Y. Hong, Anal. Chem., 2021, 93, 14996–15004.

11 M. Chung, W. H. Skinner, C. Robert, C. J. Campbell, R. M. Rossi, V. Koutsos and N. Radacsi, ACS Appl. Mater Interfaces, 2021, 13, 51504–51518.

12 X. T. Pan, Y. Y. Liu, S. Q. Qian, J. M. Yang, Y. Li, J. Gao, C. G. Liu, K. Wang and X. H. Xia, ACS Appl. Mater Interfaces, 2021, 13, 19023–19030.

13 Z. Zhao, Q. Li, Y. Dong, J. Gong, Z. Li and J. Zhang, Sens. Actuators B Chem., 2022,535, 131145.

14 U. Mogera, H. Guo, M. Namkoong, M. S. Rahman, T. Nguyen and L. Tian, Sci. Adv, 2022, 8, abn1736.